Kinetics of Methane Hydrate Formation from Polycrystalline Deuterated Ice

Xiaoping Wang,[†] Arthur J. Schultz,*[,†] and Yuval Halpern[‡]

Intense Pulsed Neutron Source and Energy Systems Division, Argonne National Laboratory, Argonne, Illinois 60439

Received: January 24, 2002; In Final Form: May 15, 2002

The kinetics of methane hydrate formation was investigated by in-situ time-of-flight neutron powder diffraction. Samples were prepared from deuterated ice particles (< 0.25 mm) and transformed to clathrate hydrate by pressurizing the system with methane gas. The rates of sI methane hydrate formation were measured in-situ under isothermal conditions with a methane pressure of 1000 psi (6.9 MPa). Kinetic data were analyzed in terms of a shrinking core model, including possible contributions of nucleation, methane diffusion, and interface reaction. The data support the hypothesis that methane hydrate formation reaction from ice particles is diffusion-controlled. The reaction starts quickly at the nucleation stage, which propagates to form a hydrate layer that covers the ice particle. Further reaction is limited by the growth of the hydrate layer and inward diffusion of methane molecules through the hydrate layer to the unreacted ice core. The reaction rate at the interface between hydrate and unreacted ice particle is fast compared to that of methane diffusion. The conversion of ice particle to methane hydrate follows Arrhenius behavior, from which an activation energy of 14.7(5) kcal/mol was derived. Complete transformation of ice to methane hydrate was achieved through temperature ramping—a nonisothermal procedure that involves slowly increasing the sample temperature through the ice melting point.

Introduction

It has been estimated that methane hydrate is the largest reservoir of fossil hydrocarbon in Earth.[1,2] It crystallizes in space group *Pm*3*n*, labeled structure I (sI), in which the methane molecules are enclathrated in pentagonal dodecahedral (5^{12}) and tetrakaidecahedral ($5^{12}6^2$) cages made of water molecules (Figure 1a and 1b). Natural gas hydrates containing mixtures of methane and propane molecules have also been found with structure II, space group *Fd*3*m*. In sII hydrate, the guest gas molecules reside in pentagonal dodecahedral (5^{12}) and hexakaidecahedral ($5^{12}6^4$) cavities (Figure 1a and 1c).[3] A third structure, structure H (*P*6/*mmm*) hydrate, is also known.[4,5] The water molecules are tetrahedrally coordinated by hydrogen bonds in all forms of hydrates, as in ordinary ice. The guest gas molecules are linked to water molecules by van der Waals forces. Early interest in gas clathrate hydrate was initiated from the problem of natural gas pipeline blockage in suboceanic and permafrost environments. With the recent reports[1,2] that the amount of carbon in naturally occurring methane hydrate is greater than those of all fossil fuels combined in earth, gas clathrate hydrate research has moved to the possibility of methane exploitation. Methane itself is a green house gas that is twenty times more effective in causing global warming than is carbon dioxide.[6] One fundamental question to be addressed is the role that dissociation and formation of gas hydrates would play in the global climate environment.

The methane hydrate phase diagram is shown in Figure 2.[5,7] Formation of methane hydrate requires elevated pressure and temperatures close to the ice melting point. Most observations on gas hydrates have been based on measurements of hydrate thermodynamic properties,[5] although diffraction techniques have been used extensively for structural studies of gas hydrates. For example, the structure of methane hydrate has been studied by X-ray and neutron diffraction in detail.[8] However, only a few reports on methane hydrate formation kinetics are found in the literature with the focus mainly on systems containing agitated liquid water.[9,10] With ice as the starting material, Holder and co-workers have shown that the growth rate of methane hydrate on large (~10 cm diameter) ice-coated stainless steel disks is inversely proportional to the thickness of the hydrate layer.[11] Stern and co-workers have reported the complete conversion of metastable (superheated) ice grains to methane hydrate by warming the sample to nearly 290 K under pressure, although these reports to do not include an analysis of reaction kinetics.[12−15]

We previously reported a study of the kinetics of the formation from ice of carbon dioxide hydrate, with structure type sI, using the High Intensity Powder Diffractometer (HIPD) and a custom-built pressure cell at the Intense Pulsed Neutron Source, Argonne National Laboratory.[16] A similar experimental setup was also used to investigate the formation of argon hydrate, with structure sII, and its transformation to structure sI by immersion in liquid CO_2.[17] In this paper, we report the reaction kinetics for the in-situ formation of methane hydrate from polycrystalline ice.

Experimental Procedures

Sample Preparation and Data Collection. Powdered ice was prepared by freezing deuterated water (Aldrich, 99.9%) in liquid nitrogen. The use of D_2O instead of H_2O for the neutron experiment is to avoid incoherent scattering background generated by H atoms. The ice was then crushed with a mortar and pestle. Large ice particles were removed through a 250-μm sieve, and the powdered ice was placed in the pressure cell that was already cooled in liquid nitrogen. The apparatus has been

* To whom correspondence should be addressed. E-mail: ajschultz@anl.gov.
[†] Intense Pulsed Neutron Source.
[‡] Energy Systems Division.

10.1021/jp025550t CCC: $22.00
Published on Web 07/18/2002

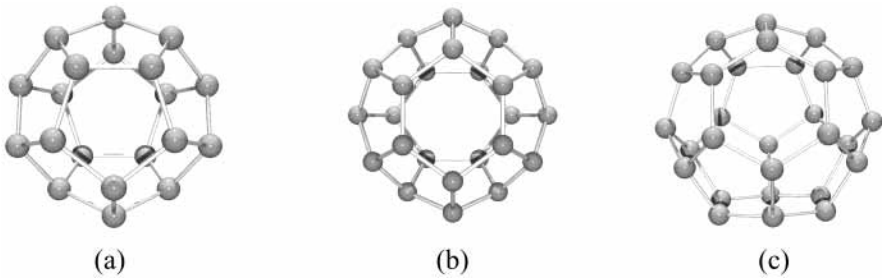

Figure 1. Cavities found in sI and sII clathrate gas hydrate: (a) 5^{12}, (b) $5^{12}6^2$, and (c) $5^{12}6^4$. The spheres represent water oxygen atoms and the rods represent disordered O−D···O ⇆ O···D−O hydrogen bonds.

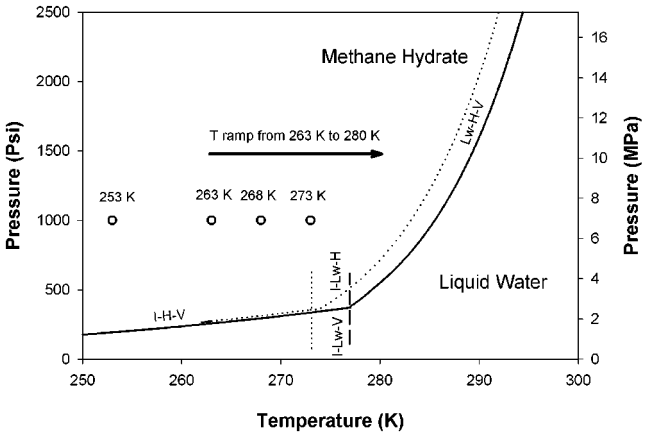

Figure 2. Phase diagram of methane hydrate. The phase diagram for CH_4-H_2O (dotted line) based on data from Sloan, p 167.[5] The phase diagram for CH_4-D_2O (solid line) was obtained by shifting the equilibrium temperature of the previous plot by +2.5 K to reflect deuterium isotopic effect.[7] (circles: P−T conditions for isothermal experiments; arrowed line: conditions for isobaric T-ramp experiment. I, ice; Lw, liquid water; V, methane vapor; H, hydrate).

described in more detail in an earlier publication.[16] Although the ice particle size was not bracketed by the use of a second sieve, the reproducibility of experiments[16] and the linear Arrhenius plots (vide infra) indicate that the particle size distribution is reproducible, which is the important factor in these analyses. The pressure cell was closed, mounted on the cold stage of a Displex closed-cycle helium refrigerator, and placed into the sample chamber on the HIPD diffractometer. The pressure cell was kept at a temperature below 240 K throughout this process to prevent the ice from melting. Before methane gas was introduced to the system, the sample was allowed to stabilize at the working temperature (253, 263, 270, or 273 K). The cell was then charged to 1000 psi (6.9 Mpa) with methane gas. We have found that it is acceptable to use hydrogenated methane (CH_4 99.99%) for neutron diffraction studies if the pressure is less than 2000 psi. Higher methane pressure in the sample container produced significantly higher incoherent scattering background from methane hydrogen atoms, making it difficult to observe the diffraction peaks. Limited instrument beam time did not allow for the measurement of complete conversion to hydrate under these conditions. Mole conversion of ice to methane hydrate in these experiments usually reached a range of 42% to 71%. Complete conversion of ice to hydrate was achieved by temperature ramping—a nonisothermal procedure that slowly ($\sim$1.4 K h^{-1}) increases the sample temperature above the ice melting point. Samples for the temperature ramp experiment were prepared in the same way as that for the isothermal experiments, and a methane pressure of 1500 psi (10.3 Mpa) was applied in the whole temperature range 263−280 K.

Neutron diffraction data were collected in 15-min intervals starting with the initial introduction of the gas into the system to observe the transformation from ice to sI methane hydrate. The total length of the data collection depended on the initial starting temperature, with longer times required at lower temperatures. Time-of-flight neutron powder diffraction data were obtained using the 90° data bank on the HIPD. The HIPD instrument has a short initial flight path (moderator-to-sample) of 5.5 m and a secondary flight path (sample-to-detector) of 1 m. This gives a higher incident neutron flux at the expense of resolution with respect to other diffractometers available at IPNS.[18]

Data Analysis. Neutron data were analyzed by Rietveld refinement using the GSAS program.[19] The lattice parameters of the phases observed in the spectrum—methane hydrate, ice, and aluminum—were refined in the initial stages but then fixed since the temperature and pressure of the sample did not change. The atomic positions and thermal parameters were determined in separate experiments for each temperature and were not varied during the refinements. In addition to four background parameters, only the histogram scale factor, an absorption coefficient, and the phase fractions were allowed to refine. The weight fractions were extracted from each refinement and plotted in terms of mole fractions of methane hydrate.

Results & Discussion

Neutrons easily penetrate certain metals such as aluminum, which allows for the use of high-pressure aluminum cell and cryogenic devices for diffraction studies. The unique setup of the high-intensity neutron powder diffractometer (HIPD) has made it convenient to follow the in-situ structural changes that occur during hydrate formation.[16]

The methane hydrate formation experiments were performed at temperatures of 253, 263, 270, and 273 K under isothermal conditions, as shown in Figure 2. Figure 3 shows a typical neutron diffraction pattern after a 51-h reaction at 273 K as a mixture of the deuterated ice starting material and the converted methane hydrate. The diffraction patterns were collected in time periods of 15 min. Plots showing the time dependence of the mole fraction of hydrate formed at four different temperatures are given in Figure 4. The conversion of ice to methane hydrate, under constant pressure and static conditions, is a temperature- and time-dependent process. The reaction rates, indicated by the slopes of individual plot versus time, show a fast initial rate at the reaction temperature. After that, the rates decrease smoothly with reaction time.

Kinetic Model for Methane Hydrate Formation under Isothermal Conditions. A kinetic model has been reported involving gas diffusion through a growing methane hydrate layer on large, flat ice surfaces maintained at or slightly above 0 °C.[11]

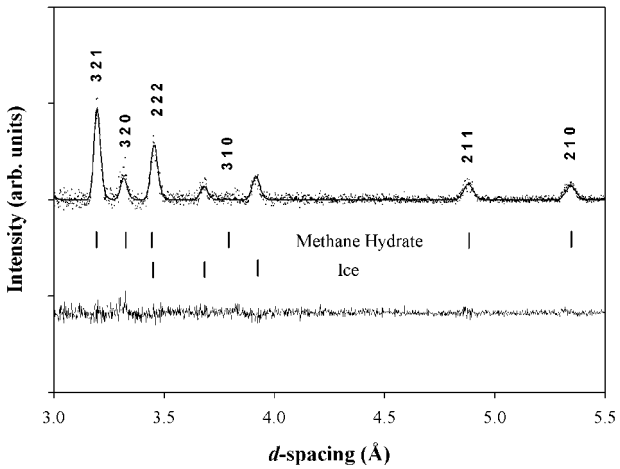

Figure 3. Portion of a 15-min neutron scattering pattern showing ice Ih particles converting to sI hydrate after a 51-h reaction at 273 K. The observed data are shown as dotted cross, and calculated intensities from Rietveld analysis are shown as a solid line, which corresponds to 72% mole conversion of ice to sI methane hydrate. The bottom line presents the difference pattern.

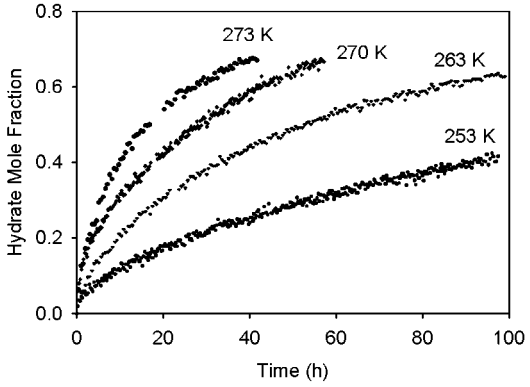

Figure 4. Conversion of deuterated ice to methane hydrate at a pressure of 1000 psi at temperatures of 253 K, 263, 270, and 273 K. Each data point represents the mole fraction of hydrate refined from a 15-min histogram. Uncertainties are approximately ±0.02 or similar in magnitude with the observed scatter of the points from a smooth curve.

In ice grains, a shrinking core model involving diffusion of methane gas through an outer mantle of hydrate to react with the inner core of ice has been postulated primarily on the basis of visual observations.[13−15]

We previously reported the formation of CO_2 hydrate under isothermal conditions,[16] and the reaction kinetics were analyzed using the simplest form of a shrinking core model[20,21] developed for gas−solid, liquid−solid, and solid−solid reactions. This model was also successfully applied to the kinetics of the formation of argon hydrate from ice and for the transformation of Ar hydrate (sII) to a mixed gas Ar/CO_2 hydrate (sI).[17] As first proposed in 1927,[22] the initial model consists of a sphere of radius r of solid phase A that is reacting with a mobile phase B (either a gas, liquid, or solid powder) to form a product layer that completely covers the sphere of A as the reaction proceeds. At a given temperature, the product thickness l was assumed to be inversely proportional to the reaction rate

$$\mathrm{d}l/\mathrm{d}t = k/l \tag{1}$$

Integration of eq 1 gives

$$l^2 = 2kt \tag{2}$$

The volume of unreacted material at time t is given as

$$V = \frac{4\pi}{3}(r - l)^3 \tag{3}$$

and

$$V = \frac{4\pi}{3}r^3(1 - \alpha) \tag{4}$$

where r is the radii of the ice particle and α is the fraction of the original sphere which has reacted. Equating the right sides of eq 3 and eq 4 produces

$$l = r(1 - (1 - \alpha)^{1/3}) \tag{5}$$

Substituting eq 5 into eq 2 gives the following equation[22]

$$t = \frac{r^2}{2k}(1 - (1 - \alpha)^{1/3})^2 \tag{6}$$

This model assumes that an initial layer of product forms quickly after the solid phase A is exposed to the mobile reactant B. Once a product layer is formed on A, the reaction becomes diffusion-controlled and the reaction kinetics can be analyzed with eq 6. In some cases, the propagative surface nucleation growth may take a measurable amount of time t^*, after which time the hydrate formation is diffusion-controlled. According to Fujii and Kondo,[23] eq 7 can be derived when the time t^* and the corresponding mole conversion of the reactant, α*, are considered:

$$(1 - \alpha)^{1/3} = \frac{-(2k)^{1/2}}{r}(t - t^*)^{1/2} + (1 - \alpha^*)^{1/3} \tag{7}$$

A linear relationship can be found between $(1-\alpha)^{1/3}$ and $(t - t^*)^{1/2}$ for a suitable value of t^* and α* which give the best fit to the observed data using eq 7. For a given particle size, the diffusion constant k can be calculated from the slope of the straight line. The parameter t^* represents the time when the conversion process is initially dominated by the diffusion of guest molecules through the hydrate layer. In the previously reported CO_2 hydrate experiments,[16] the time t^* was selected corresponding to ∼22% conversion at each reaction temperature. This produced the best linear fit of eq 7 to the data obtained in the temperature range 230−263 K. For a given particle size distribution at these temperatures, the reaction follows Arrhenius behavior $k = A\exp[-E_a/(RT)]$, where R is the gas constant. If k_{eq7} is defined as k/r^2, k_{eq7} can be calculated for each temperature and an activation energy of 6.5 kcal/mol was calculated from the linear plot of $\ln(k_{eq7})$ against $1/T$ for CO_2.[16]

Since eq 7 has been used successfully for the CO_2 hydrate formation process, a similar analysis has been applied to the methane hydrate formation reaction. Figure 5 presents the best fit of the data with the time t^* corresponding to 10% conversion. The linear correlation coefficients R_{fit} range from 0.988 to 0.997 (Table 1), indicative of good fits of the data to eq 7. However, it can be seen that there are systematic deviations from the straight lines for all four curves, especially in the low α region.

The models for eqs 6 and 7 are limited in part because they are based on the assumption that the reaction proceeds on a plane surface. To overcome the limitation of this assumption, a more complex model for gas solid reaction is adopted to analyze the kinetics of methane hydrate formation that includes a spherical surface and other reaction steps in addition to diffusion. In the more complex shrinking core model,[24−26] the overall

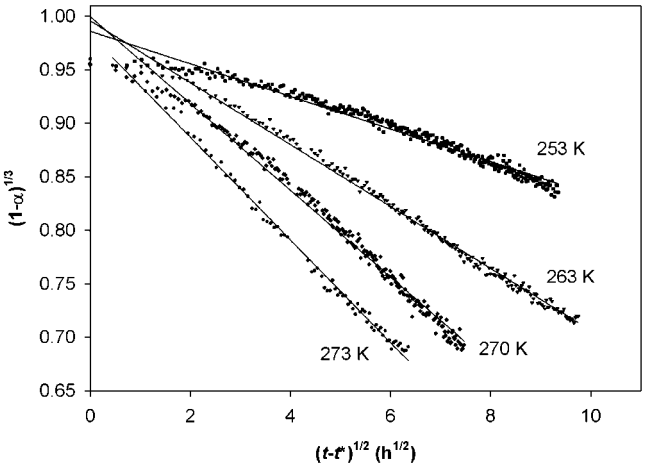

Figure 5. A plot of the fit of experimental data in terms of the shrinking core model based on eq 7.

TABLE 1: List of the Results for Isothermal Experiments

	eq 7		eq 10	
temperature, K	$k_{eq7}{}^a \times 10^4$	$R_{fit}{}^b$	$k_{eq10}{}^a \times 10^4$	$R_{fit}{}^b$
253	1.15	0.988	1.14	0.990
263	4.18	0.996	3.42	0.997
270	8.20	0.994	6.35	0.997
273	11.52	0.997	10.11	0.992
E_a, kcal mol^{-1}	15.7 ± 0.5		14.7 ± 0.5	

[a] $k_{eq7} = k/r^2$ in eq 7. $k_{eq10} = 1/(6\tau)$ in eq 10. [b] Linear correlation coefficient.

reaction of methane with ice particle consists of three stages: (a) initial reaction of methane with the surface of ice particle, with time constant τ_1; (b) growth of hydrate layer and inner diffusion of methane gas, with time constant τ_2; (c) reaction of methane gas with ice at the unreacted ice core, with time constant τ_3. If the three steps occur in series, then the mole fraction of methane hydrate formed at reaction time t can be expressed according to the following equation:[25,26]

$$t = \tau_1(1 - (1 - \alpha)^{2/3}) + \tau_2(1-3(1 - \alpha)^{2/3} + 2(1 - \alpha)) + \tau_3(1 - (1 - \alpha)^{1/3}) \quad (8)$$

Thus, the time (τ_{total}) needed for complete conversion of ice particle to methane hydrate ($\alpha = 1$) equals the sum of the three time constants:

$$\tau_{total} = \tau_1 + \tau_2 + \tau_3 \quad (9)$$

As a test, values of τ_1, τ_2, and τ_3 were derived from least-squares fit of eq 8 to a plot of $(1 - \alpha)$ versus t. From this fit, it was found that τ_1 and τ_3 are quite small compared to the time constant of the diffusion-controlled process, τ_2.

Thus, the above equation can be abbreviated to the diffusion-limited kinetic equation

$$t = \tau_2(1-3(1 - \alpha)^{2/3} + 2(1 - \alpha)) \quad (10)$$

where t is reaction time and α is the mole fraction of reacted ice, while $\tau_2 = r^2\rho/6bD_eC_B$, where r is the particle radius, D_e is the diffusion coefficient of B in the hydrate layer, C_B is the concentration of B at the ice particle (A) surface, ρ is the molar density of the particle (deuterated ice, 0.052 mol/cm^3, at 0 °C and 1 atm), and b is the stoichiometric ratio of moles of A reacted per mole of B (5.8 for methane hydrate). This model has been used recently in the study of ice particle conversion to ammonia hemihydrate.[27]

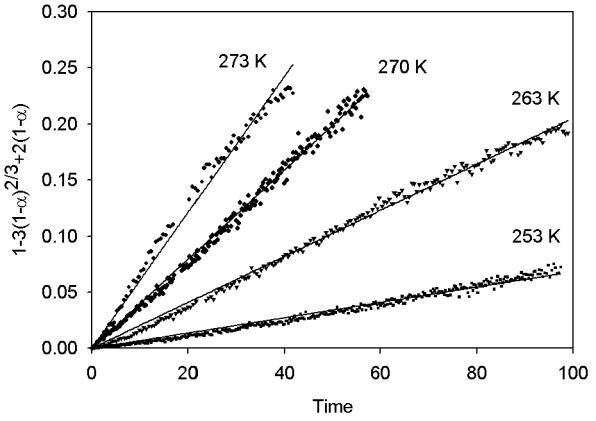

Figure 6. A plot of the fit of experimental data in terms of the shrinking core model based on eq 10.

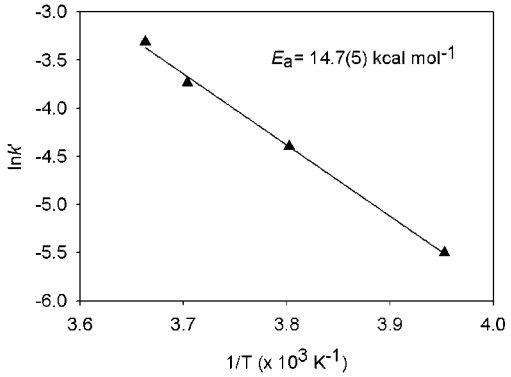

Figure 7. A plot of ln(k′) as a function of $1/T$ (K^{-1}) for eq 10. Activation energy for the diffusion process to form methane hydrate was calculated from the slope of the line fits.

Comparison of the correlation coefficients R in Table 1 for eqs 7 and 10 indicate that both models fit the data equally well. Furthermore, comparison of the R_{fit} values for eq 8 and eq 10 also supports the hypothesis that the rate of diffusion is the controlling factor since including the other terms in eq 8 does not lead to any improvement (the R_{fit} values are already almost equal to 1.0).

Figure 6 presents the comparison of the experimental and calculated mole fractions versus time data for the methane hydrate formation reaction at various temperatures of the kinetic study using eq 10. The diffusion constants depend on the particle size and temperature, but for a given particle size distribution, the activation energy of the diffusion process is independent of these variables. If k_{eq10} is defined as $bD_eC_B/r^2\rho$, it can be calculated from the fits in Figure 6 for each temperature; the results are listed in Table 1. The temperature dependence of a thermally dependent diffusion process should follow Arrhenius behavior described by $k_{eq10} = A \exp[-E_a/(RT)]$, where R is the gas constant.

Figure 7 shows the straight line obtained by plotting lnk_{eq10} against $1/T$. An activation energy value of 14.7(5) kcal/mol was calculated from the slope of this line. This is greater than the energy needed to break the hydrogen bonding in ice (12.7 kcal/mol)[28] and the energy needed to break the hydrogen bonding in liquid water (5 kcal/mol). The activation energy of 14.7(5) kcal/mol for methane hydrate formation is also greater than our previous results in the CO_2 hydrate system, which had an E_a of 6.5 kcal/mol,[16] but is smaller than the activation energy for the dissociation of methane hydrate, which was reported to be 19.4

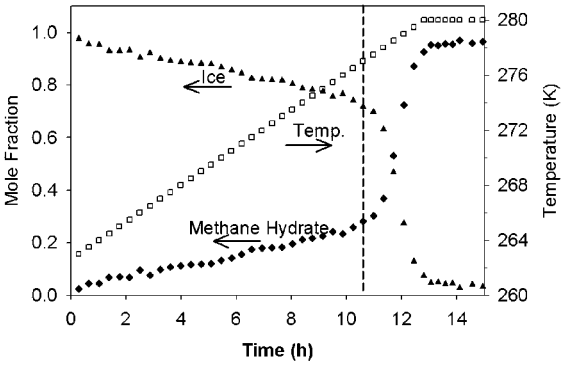

Figure 8. Conversion of deuterated ice to sI methane hydrate through temperature ramp at 1500 psi. Vertical dashed line is the melting point of D_2O ice (277 K).

kcal/mol.[29,30] The kinetic measurement results are in agreement with a diffusion-controlled process that occurs between methane molecules and the hydrate layer that grows toward the inner core of ice particle. Although direct transformation of ice into liquid water is not a prerequisite for hydrate formation, we cannot rule out the possibility that a quasi-liquid layer exists between the hydrate layer and the unreacted surface of ice particle. The quasi-liquid layer is believed to be a thin mobile phase of water molecules with mobilities intermediate between those of liquid water and crystalline ice.[31]

Nonisothermal Methane Hydrate Synthesis. With the increased interest in methane hydrate research, it is important to be able to prepare methane hydrate under controlled conditions that ensure replicability. Methane hydrate formation from ice is a slow process at low temperature, where complete conversion of ice into hydrate crystals can take days. Thus, it is not practical to synthesize pure methane hydrate at low-temperature conditions. As shown in Figure 2, the equilibrium pressure for CH_4/H_2O hydrate at 280 K is 736 psi (5.07 MPa), as calculated using the CSMHYD program provided by Sloan.[5] Deuterated ice has a melting point of 276.9 K, which is about 3.8 K higher than H_2O. As a result of the isotope effect, methane hydrate formed from D_2O would be expected to be stable at temperatures of 2−4 K higher than that of the H_2O hydrate, similar to equilibrium temperatures reported for CO_2 hydrates with H_2O and D_2O.[7] As shown in the phase diagram in Figure 2, methane hydrate is stable in D_2O at 280 K with a methane pressure of over 490 psi (3.5 MPa). Thus, it is possible to prepare the hydrate by increasing the sample temperature through the deuterated ice melting point analogous to previous reports with H_2O ice.[12−15]

Methane hydrate formation from deuterated ice under nonisothermal condition was monitored in-situ with the HIPD instrument. With the sample maintained at constant pressure (1500 psi), the temperature was increased slowly (1.4 K/h) from 263 to 280 K. The plot of mole fraction of hydrate formed versus temperature is shown in Figure 8. The reaction rates change significantly as the temperature reaches the ice melting point. Although there is a sharp increase of reaction rates above the ice melting point, the neutron diffraction data show that the ice particles do not immediately melt but apparently exist for nearly 2 h as the temperature is slowly ramped from 277 to 280 K (Figure 8). Complete conversion to methane hydrate is achieved after continued warming of the sample to 280 K, where the ice diffraction peaks disappear and the intensities of methane hydrate peaks remain unchanged thereafter.

These observations are consistent with observations of superheated ice during temperature ramping by Stern and co-workers,[12−15] who prepared methane hydrate at higher pressure (∼30 MPa) and temperature (∼290 K). The reaction was monitored by carefully recording the pressure−temperature history during sample fabrication and by the use of an optical cell to visually observe the hydrate formation reaction during temperature ramping. It was found that hydrate growth is rapid on ice grains after initial exposure to methane gas. However, this growth appeared limited until continued warming of the sample to above the ice melting point. Full conversion to methane hydrate was achieved at temperatures approaching 290 K in 6−8 h, and no bulk melting of ice grains or free liquid water was detected until the hydrate decomposition conditions (292 K and 30 MPa) was reached.[13]

Neutron diffraction shows the in-situ time dependence of diffraction patterns for ice and methane hydrate in the sample cell in the temperature range 263−280 K. From Figure 8, it is seen that ice is present above its melting point and that it appears to be consumed at the same, but opposite, rate as the amount of hydrate increases. These results are in agreement with the hypothesis that free liquid water phase is not required for converting ice into gas hydrate and appear to demonstrate the existence of superheated ice. However, whereas the observations of superheated ice by Stern and co-workers[12−15] were obtained with pressures of 27−33 MPa and temperatures of ∼290 K for 8−12 h, our neutron diffraction measurements were at ∼10 MPa with slow ramping to 280 K (only 3 K above the D_2O melting point) within a 2 h period (Figure 8). Thus, a possible alternative explanation for the observation of ice above its melting point is the insulating properties of the hydrate layer,[32] which may keep the ice core cooler than the measured temperature of the sample container.

Summary

The hydrate formation reaction was performed under both isothermal and nonisothermal conditions. For reactions at temperatures of 253, 263, 270, and 273 K and methane pressure of 1000 psi, the reaction kinetics are analyzed with various forms of a shrinking core model. This analysis is consistent with a mechanism for which the rate of methane hydrate formation from ice particles is diffusion-controlled. In this proposed model, the reaction starts quickly at the nucleation stage, which propagates to form a hydrate layer that covers the ice particle completely. Further reaction is limited by the growth rate of the hydrate layer and inward diffusion of methane molecules through the hydrate layer to the unreacted ice core. An activation energy of 14.7(5) kcal/mol was obtained for the conversion of ice particles to methane hydrate. Reaction of methane with deuterated ice particles during temperature-ramping process was also investigated by the in situ neutron diffraction technique. The neutron diffraction data exhibit peaks from ice at temperatures above the ice melting point until nearly 100% of the ice is converted to methane hydrate at 280 K.

Acknowledgment. The work at Argonne National Laboratory was supported by the U.S. Department of Energy, Basic Energy Sciences-Material Sciences, under Contract No. W-31-109-ENG-38.

References and Notes

(1) Haq, B. U. In *Science*; 1999; Vol. 285, pp 543−544.

(2) Max, M. D. *Natural Gas Hydrate: In Oceanic and Permafrost Environments*; Kluwer Academic Publishers: Boston, 2000.

(3) Jeffrey, G. A.; McMullan, R. K. *Prog. Inorg. Chem.* **1967**, *8*, 43−108.

(4) Ripmeester, J. A.; Tse, J. S.; Ratcliffe, C. I.; Powell, B. M. *Nature* **1987**, *325*, 135−136.

(5) Sloan, E. D., Jr. *Clathrate Hydrates of Natural Gases*, 2nd ed.; Marcel Dekker: New York, 1998.

(6) *Climate Change 1995: The science of climate change*; Houghton, J. T., Meira Filho, L. G., Callander, B. A., Harris, N., Kattenberg, A., Maskell, K., Eds.; Cambridge University Press: New York, 1996.

(7) Chun, M.-K.; Yoon, J.-H.; Lee, H. *J. Chem. Eng. Data* **1996**, *41*, 1114−1116.

(8) Gutt, C.; Asmussen, B.; Press, W.; Johnson, M. R.; Handa, Y. P.; Tse, J. S. *J. Chem. Phys.* **2000**, *113*, 4713−4721.

(9) Malegaonkar, M. B.; Dholabhai, P. D.; Bishnoi, P. R. *Can. J. Chem. Eng.* **1997**, *75*, 1090−1099.

(10) Makogon, Y. F. *Hydrates of Hydrocarbons*; PennWell: Tulsa, OK, 1997.

(11) Hwang, M. J.; Wright, D. A.; Kapur, A.; Holder, G. D. *J. Inclusion Phenom. Mol. Recognit. Chem.* **1990**, *8*, 103−116.

(12) Stern, L. A.; Kirby, S. H.; Durham, W. B. *Science* **1996**, *273*, 1843−1848.

(13) Stern, L. A.; Hogenboom, D. L.; Durham, W. B.; Kirby, S. H.; Chou, I.-M. *J. Phys. Chem. B* **1998**, *102*, 2627−2632.

(14) Stern, L. A.; Kirby, S. H.; Durham, W. B. *Energy Fuels* **1998**, *12*, 201−211.

(15) Stern, L. A.; Kirby, S. H.; Durham, W. B. *J. Phys. Chem. A* **2001**, *105*, 122−1224.

(16) Henning, R. W.; Schultz, A. J.; Thieu, V.; Halpern, Y. *J. Phys. Chem. A* **2000**, *104*, 5066−5071.

(17) Halpern, Y.; Thieu, V.; Henning, R. W.; Wang, X.; Schultz, A. J. *J. Am. Chem. Soc.* **2001**, *123*, 12826−12831.

(18) Jorgensen, J. D.; Faber, J., Jr.; Carpenter, J. M.; Crawford, R. K.; Haumann, J. R.; Hitterman, R. L.; Kleb, R.; Ostrowski, G. E.; Rotella, F. J.; Worlton, T. G. *J. Appl. Crystallogr.* **1989**, *22*, 321−333.

(19) Larson, A. C.; Von Dreele, R. B. *GSAS--General Structure Analysis System*; Report No. LAUR 86-748; Los Alamos National Laboratory: Los Alamos, NM, 2000.

(20) FitzGerald, S. A.; Neumann, D. A.; Rush, J. J.; Bentz, D. P.; Livingston, R. A. *Chem. Mater.* **1998**, *10*, 397−402.

(21) Berliner, R.; Popovici, M.; Herwig, K. W.; Berliner, M.; Jennings, H. M.; Thomas, J. J. *Cem. Concr. Res.* **1998**, *28*, 231−243.

(22) Jander, W. *Z. Anorg. Allg. Chem.* **1927**, *163*, 1−30.

(23) Fujii, K.; Kondo, W. *J. Am. Ceram. Soc.* **1974**, *57*, 492−497.

(24) Rekoske, J. E.; Barteau, M. A. *Ind. Eng. Chem. Res.* **1995**, *34*, 2931−2939.

(25) Levenspiel, O. *Chemical Reaction Engineering*; 3rd ed.; Wiley & Sons: New York, 1999.

(26) Froment, G. F.; Bischoff, K. B. *Chemical Reactor Analysis and Design*; Wiley & Sons: New York, 1990.

(27) Uras, N.; Devlin, J. P. *J. Phys. Chem. A* **2000**, *104*, 5770−5777.

(28) Itagaki, K. *J. Phys. Soc. Jpn* **1967**, *22*, 427−431.

(29) Clark, M.; Bishnoi, P. R. *Can. J. Chem. Eng.* **2001**, *79*, 143−147.

(30) Kim, H. C.; Bishnoi, P. R.; Heidemann, R. A.; Rizvi, S. S. H. *Chem. Eng. Sci.* **1987**, *42*, 1645−1653.

(31) Mizuno, Y.; Hanafusa, N. *J. Phys., Colloq. C1 Suppl.* **1987**, *48*, 511−517.

(32) Moudrakovski, I. L.; Ratcliffe, C. I.; McLaurin, G. E.; Simard, B.; Ripmeester, J. A. *J. Phys. Chem. A* **1999**, *103*, 4969−4972.